Attenuated spread of X-inactivation in an X;autosome translocation

Bilyana C. Popova*, Takashi Tada†, Nobuo Takagi‡, Neil Brockdorff*§, and Tatyana B. Nesterova*

*Developmental Epigenetics, Medical Research Council Clinical Sciences Center, Imperial College Faculty of Medicine, Hammersmith Hospital, DuCane Road, London W12 ONN, United Kingdom; †Stem Cell Engineering, Stem Cell Research Center, Institute for Frontier Medical Sciences, Kyoto University, 53 Kawahara-cho, Shogoin, Sakyo-ku, Kyoto 606-8507, Japan; and ‡Hokusei Gakuen University, Atsubetsu-ku, Sapporo 004-8631, Japan

Communicated by Mary F. Lyon, Medical Research Council, Didcot, United Kingdom, March 14, 2006 (received for review January 20, 2006)

X inactivation in female mammals involves transcriptional silencing of an entire chromosome in response to a cis-acting noncoding RNA, the X inactive-specific transcript (*Xist*). *Xist* can also inactivate autosomal sequences, for example, in X;autosome translocations; but here, silencing appears to be relatively inefficient. This variation has been attributed to either attenuated spreading of *Xist* RNA at the onset of X inactivation or inefficient maintenance of autosomal silencing. Evidence to date has favored the latter. Here, we demonstrate attenuated spreading of *Xist* RNA at the onset of X inactivation in the T(X;4)37H X;autosome translocation. Our findings provide direct evidence that underlying chromosome/chromatin features can disrupt spreading of the primary inactivating signal.

line-1 | *Xist*

X inactivation is the dosage compensation mechanism in female mammals. In early embryogenesis both X chromosomes are active. Transcriptional silencing of a single X chromosome then proceeds, coincident with the onset of cellular differentiation. Normally X inactivation occurs randomly, there being an equal probability that either the maternally or paternally derived X chromosome will be inactivated in a given cell. The inactive state is stable and is maintained through subsequent cell divisions (reviewed in ref. 1).

X inactivation is regulated by a single cis-acting master control locus, the X inactivation center (Xic). The Xic transcribes a noncoding RNA, the X inactive-specific transcript (*Xist*), which associates along the length of the chromosome from which it is transcribed (2–7). Spreading of *Xist* RNA leads to conversion of the chromosome to a silent heterochromatic configuration. This X inactivation involves multiple epigenetic changes, including covalent modification of core histone tails, incorporation of variant histones, and DNA methylation (reviewed in ref. 8).

It is important to understand how *Xist* RNA propagates or spreads from the Xic along the entire length of the X chromosome. Classical genetic analysis of X;autosome (X;A) translocations has demonstrated that autosomal loci linked *in cis* to the Xic are inactivated less efficiently than normal X-linked genes (9, 10). It has been suggested that this variation is due to either attenuated spreading of silencing at the onset of X inactivation in early development or failure to efficiently maintain autosomal silencing through ontogeny, referred to as "spread and retreat." These two models are not mutually exclusive, but evidence to date favors spread and retreat. Specifically, studies using Cattanachs' translocation, Is(X;7)1ct, an insertion of a region of chromosome 7 into the X chromosome, demonstrated initial spread and subsequent retreat of silencing at the *albino* (*c*) locus present within the insertion (10). Additionally, studies using *Xist* transgenes located in autosomes have reported efficient spread of *Xist* RNA (11, 12), which does not support the argument for the "attenuated spread" model. Set against this background, indirect cytogenetic analysis of X inactivation spreading in mouse embryos carrying the balanced T(X;4)37H (T37H) translocation, by using either Kanda staining (13) or late replication analysis (14), indicates that spread into autosomal material is attenuated in early development, soon after the onset of random X inactivation.

To account for increased efficiency of silencing on the X chromosome relative to autosomes, Gartler and Riggs (15) proposed the idea of "way stations" or "booster elements" that facilitate spreading (and/or maintenance) of X inactivation. These elements are predicted to be unique to, or at least more prevalent on, the X chromosome. More recently, Lyon (16) suggested that LINE-1 (L1) repetitive elements, which are present at a relatively high density on the X chromosome, are candidates for way stations. This idea is broadly supported by analyses of human genome sequence showing that L1 density on the X chromosome is approximately twice the genome average (17, 18). L1 density is especially high around the human XIC locus, consistent with a role in spreading of the signal (17). Conversely the density is closer to the genome average around genes that are known to escape X inactivation (18), again supporting a role for L1s in X inactivation.

Our previous studies, analyzing translocation bearing fibroblast cell lines derived from adult T37H females, found that *Xist* RNA and also histone hypoacetylation show only limited spread into chromosome 4 material (19). Similar results were obtained by others looking at X;A translocations in human cells (20–23). In all of these cases, the cells analyzed came from adult animals/tissues, and the results, therefore, do not discriminate between attenuated spread at the onset of X inactivation versus spread and retreat. To overcome these limitations, we have used T37H XX ES cells, allowing us to analyze spread of *Xist* RNA and associated silencing marks at the time when X inactivation is first initiated. We find that linear spread is, indeed, attenuated at the onset of X inactivation in T37H, generally failing to progress much beyond the translocation breakpoint. We show that this finding correlates with the presence of an exceptionally large (20 Mb) L1-depleted/gene-rich region on chromosome 4, beginning at the translocation breakpoint. We discuss these results in the context of understanding the mechanism of spread of *Xist* RNA.

Results

Characterization of a Stable XX ES Cell Line Carrying the T37H Translocation. To discriminate between attenuated-spread and spread-and-retreat models, we set out to analyze an XX ES cell line, TMA-2, bearing the T37H translocation (24). XX ES cells provide a useful model for analyzing early stages of X inactivation, because both X chromosomes are active in undifferentiated cells, but *Xist* expression and random X inactivation are induced in response to differentiation *in vitro* (5).

Illustrations of the T37H translocation (25), together with probes and markers used in this study, are shown in Fig. 1 *A–C*. The TMA-2 ES cells were found to be karyotypically unstable, showing frequent loss of an X chromosome, a problem that

Conflict of interest statement: No conflicts declared.

Abbreviations: BAC, bacterial artificial chromosome; RT, room temperature; X;A, X;autosome; Xic, X inactivation center, 4^{Xi}, inactive 4^{X}.

§To whom correspondence should be addressed. E-mail: neil.brockdorff@csc.mrc.ac.uk.

www.pnas.org/cgi/doi/10.1073/pnas.0602021103

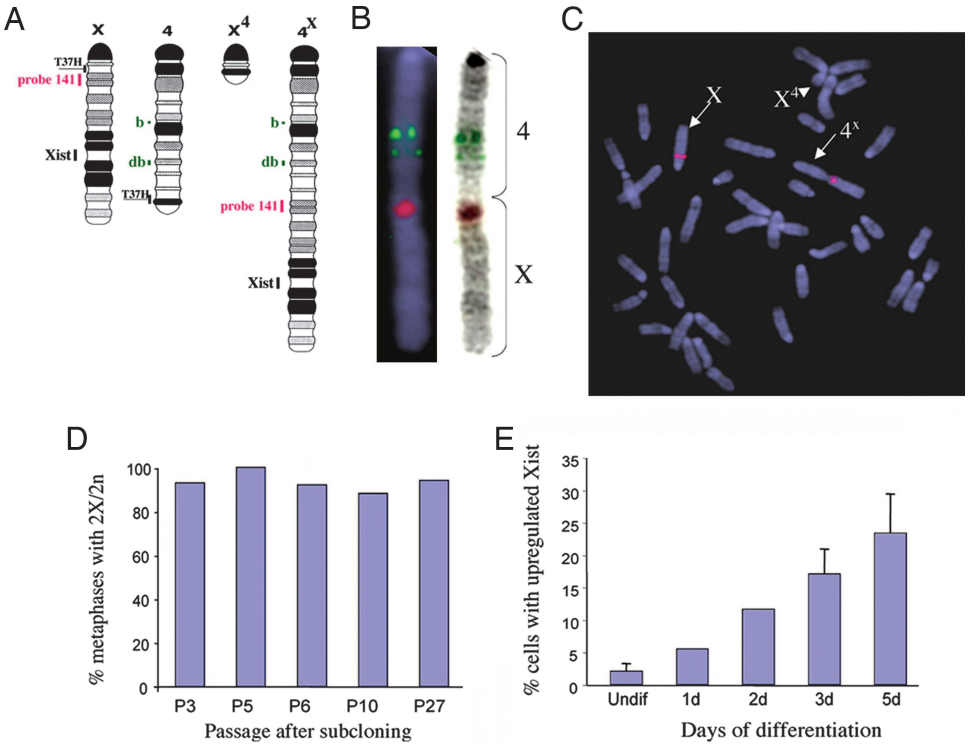

Fig. 1. Characteristics of TMA-2 ES cells carrying the T37H translocation. (*A*) Ideogram of the mouse chromosomes X and 4 and the X^4 and 4^X translocation products in the T37H translocation. Approximate location of the T37H translocation breakpoint, *Xist*, *brown* (*b*) and *diabetes* (*db*) loci as well as X-specific 141 probe are shown. (*B*) Localization of *db* and *b* loci (green) and X-specific 141 repeat (red) on 4^X product in T37H translocation. The chromosome is counterstained with DAPI (blue). Computer-generated, G-like banding of the same chromosome based on DAPI staining is shown alongside. Brackets indicate chromosome X and 4 parts. (*C*) An example of a metaphase spread illustrating X^4 (arrowhead) and 4^X (arrow) T37H translocation products in comparison with the normal X chromosome (arrow). X-specific 141 probe (red) is used for chromosome identification. (*D*) Analysis of karyotype stability of TMA-2/S8 clone. Preservation of both normal X and 4^X chromosomes was analyzed by DNA FISH with X chromosome paint at passages 3, 5, 6, 10, and 27 (P3, P5, P6, P10, and P27, respectively). (*E*) Dynamics of X inactivation in TMA-2/S8 ES cell differentiation analyzed by *Xist* RNA accumulation in differentiating cells at days 1, 2, 3, and 5.

occurs relatively commonly in XX ES cell lines (26). However, we were able to identify a stable subline, TMA-2/S8, after serial subcloning. TMA-2/S8 cells showed the correct T37H XX karyotype in ≈90% of mitotic indexes, and stability was retained after multiple passages (Fig. 1*D*).

To determine the dynamics of X inactivation in TMA-2/S8 cells, we carried out interphase RNA FISH analysis of *Xist* expression at various time points after initiation of *in vitro* differentiation. The results, shown in Fig. 1*E*, demonstrate that the number of *Xist*-expressing cells increases progressively between days 2 and 5 of differentiation, reaching a maximum of 20–30% of cells. This result is similar to data obtained for other XX ES cell lines (27), although the maximum number of expressing cells is somewhat lower. TMA-2/S8 cells were found to inactivate either the 4^X translocation product or the normal X chromosome after *in vitro* differentiation. There was a bias toward inactivation of the normal X chromosome (78% of cells at 3 days of differentiation), consistent with results reported in ref. 13.

Analysis of Trimethyl Histone H3 Lysine 27 (H3K27me3), a Marker for *Xist*-Mediated Silencing. To determine the extent of spreading into autosomal material at the onset of X inactivation, we first analyzed the chromatin modification H3K27me3 on inactive 4^X (4^Xi) metaphase chromosomes. H3K27me3 on Xi is catalyzed by the polycomb repressor complex PRC2 (28), recruitment of which depends on *Xist* RNA (28–30). This modification, therefore, provided us with a surrogate marker to determine whether or not X inactivation spreads onto the attached autosomal material. The extent of spread was assessed by DNA FISH analysis using markers on the X chromosome and chromosome 4 (Fig. 1 *A* and *B*). The patterns observed were categorized into four different groups: no spread into chromosome 4 material, spread as far as either the *db* or *b* marker, spread beyond the *db* and *b* markers, and complete spread over the chromosome 4 material (for further information see *Materials and Methods*). Examples of these categories are shown in Fig. 2 *A* and *B*, and the scoring data are summarized in Fig. 2*C*.

TMA-2/S8 cultures differentiated for 3–5 days have a high proportion of cells in which *Xist* up-regulation occurred during the preceding 24 h (Fig. 1*E*). If spread and retreat were occurring, we would expect to see a reasonable proportion of 4^Xi chromosomes showing spread along the entire chromosome. However, at both day 3 and day 5, the majority of 4^Xi chromosomes showed either no spread into chromosome 4 material or only limited spread up to the *db*/*b* markers (Fig. 2*C*). In the latter category, H3K27me3 signal on chromosome 4 appeared weaker than on the X chromosome (see, for example, Fig. 2*B2*). A small number of 4^Xi chromosomes showed spread beyond the *db*/*b* markers. Spread over most of the 4^X chromosome was seen in only three examples from 3-day differentiated cultures (Fig. 2*B*; and see *Discussion*). Taken together, these observations point to attenuation of initial spread of X inactivation as opposed to spread and retreat being the primary mechanism in T37H.

Attenuated spread of H3K27me3 was also seen in the T37H adult fibroblasts, consistent with our previous observations analyzing H4 hypoacetylation and *Xist* RNA localization (19). The proportions of the different categories were nearly identical to differentiating TMA-2/S8 cells, suggesting that attenuated spread at the onset of X inactivation is primarily responsible for the patterns observed in later ontogeny or after cell-line propagation.

Costaining for H4 Acetylation and H3K27me3 in Chromosome 4 Regions Subject to Limited Spread. We went on to analyze a second X inactivation-associated chromatin modification, hypoacetylation of histone H4 (AcH4), focusing on TMA-2/S8 cells differentiated for 5 days. Scoring data are summarized in Fig. 2*E*. The majority of samples showed no spread of hypoacetylation beyond the X;A translocation breakpoint. We previously reported similar results for the T37H adult fibroblast cell line (19), and these data are included in Fig. 2*E* for comparison.

We also stained metaphases for both H3K27me3 and AcH4 (Fig. 2*D*) and observed that the signals often overlap in the region immediately proximal of the translocation breakpoint. We interpret this result as indicating incomplete heterochromatin formation in the chromosome 4 region up to the *db*/*b* markers. It is possible that genes within this region are only partially repressed, as has been reported for some genes on the

DEVELOPMENTAL BIOLOGY

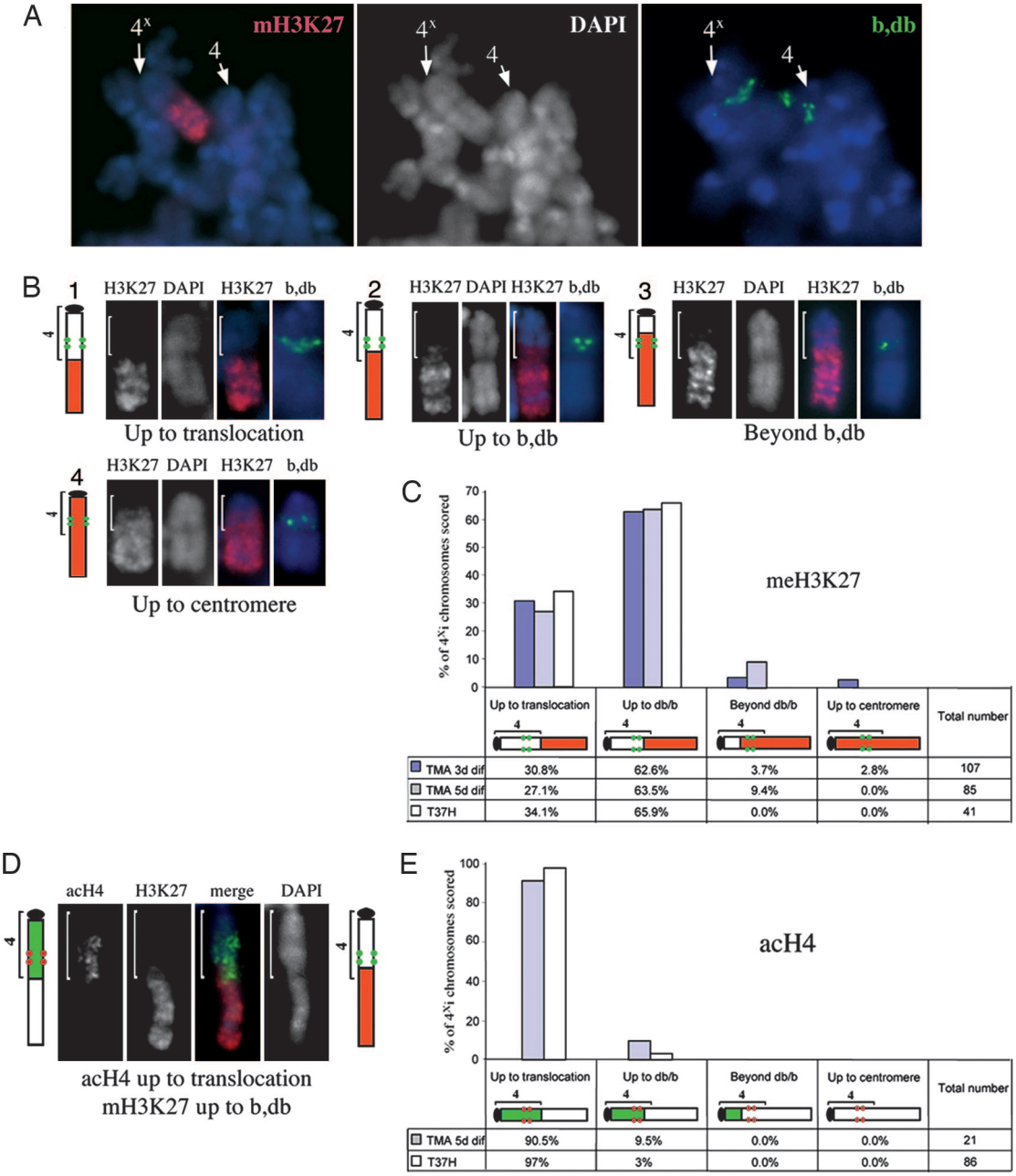

Fig. 2. Attenuated spread of chromatin modifications in T37H at the onset of X inactivation. (*A*) Metaphase chromosomes from a 5-day differentiated TMA-2/S8 cell, illustrating lack of H3K27 histone methylation in the autosomal part of 4^{X}i chromosome (*Left*). Arrows indicate chromosomes 4^{X} and 4 as identified by DNA FISH with chromosome 4 markers *brown* (*b*) and *diabetes* (*db*) (*Right*). (*B*) Representative examples of H3K27me3 staining of the 4^{X}i chromosome in differentiating TMA-2/S8 ES cells. Metaphases with H3K27me3 on the 4^{X} chromosome were classified into four categories depending on the extent of spread into chromosome 4 material: up to translocation (*B1*), up to *db*/*b* (*B2*), beyond *db*/*b* (*B3*), and up to the centromere (*B4*). Schematic shows the extent of spread for each category. The chromosome 4 constituent is indicated with a bracket, the red box illustrates the degree of H3K27me27 spread, and green circles show the position of *db*/*b* markers on chromosome 4. Each example is presented, illustrating H3K27me3 (shown in red on one panel and, to improve contrast, uncolored in another panel), position of *db*/*b* markers (green), and secondary constriction close to the translocation breakpoint (DAPI) (*C*) Summary showing percentage of cells for each category illustrated in *B*. Data are shown for TMA-2/S8 cells differentiated for 3 days (dark blue bar) and 5 days (light blue bar) and adult T37H fibroblasts (white bar). Scoring data and the number of metaphases analyzed are shown in the table (*Lower*). (*D*) Representative example of acH4 and H3K27me3 staining of the 4^{X}i chromosome in 5-day differentiated TMA-2/S8 ES cells. Schematic on the right shows the extent of 3meH3K27 spreading and schematic on the left illustrates the extent of H4 hypoacetylation (white box). Note that there is a region of overlap between 3meH3K27 and acH4 corresponding approximately to the region between translocation breakpoint and *db*/*b* markers. (*E*) Summary of H4 hypoacetylation analysis in 5-day differentiated TMA-2/S8 ES cells. Metaphases with a 4^{X}i chromosome were categorized as in *B* and *C*. Scoring data and the number of metaphases analyzed are shown in the table (*Lower*). Data for T37H somatic cells are from Duthie *et al.* (19) and are included for comparison.

X chromosome that escape X inactivation (reviewed in ref. 1) or, alternatively, that chromatin silencing occurs at selected sites in this region, whereas other genes remain fully active.

Attenuated Spread of *Xist* RNA at the Onset of X Inactivation. To confirm our observation that the T37H translocation presents a block to the initial spread of X inactivation, we went on to analyze

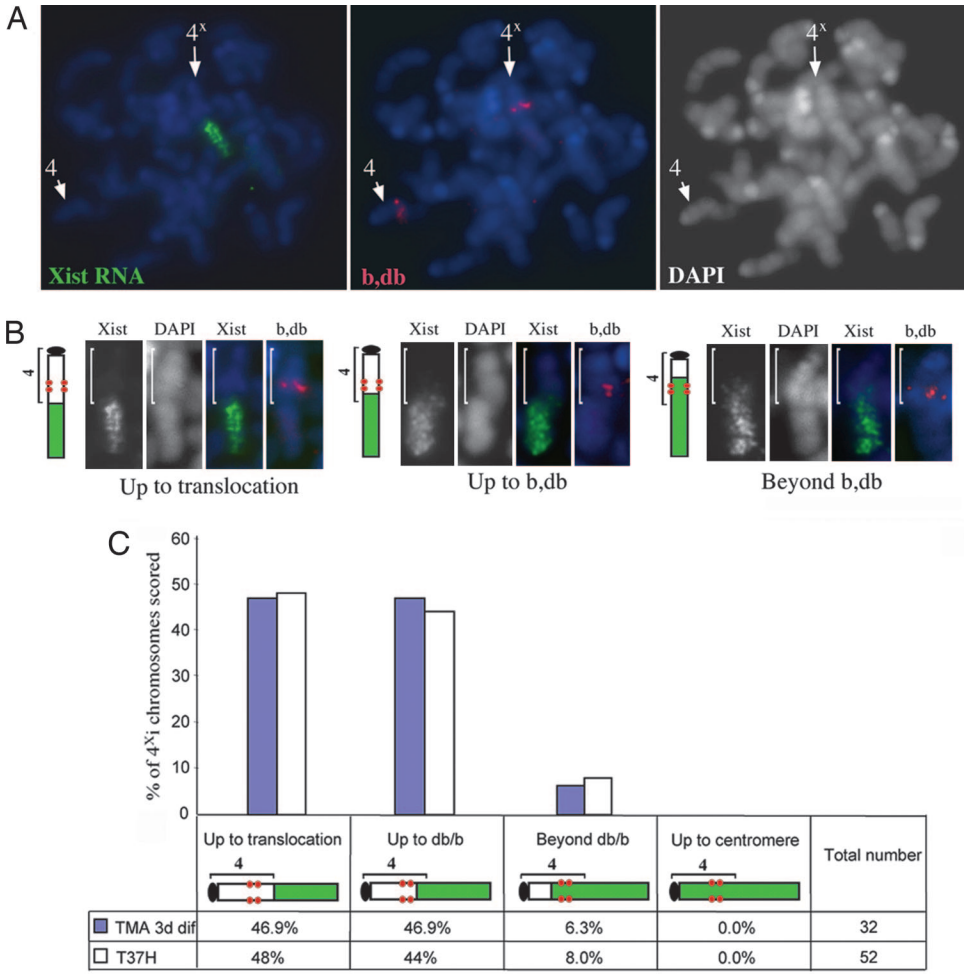

Fig. 3. Spreading of *Xist* RNA in T37H is attenuated at the onset of X inactivation. (*A*) Metaphase chromosomes from a 3-day differentiated TMA-2/S8 cell after RNA FISH with *Xist* probe (*Left*, green), followed by DNA FISH with *brown* (*b*) and *diabetes* (*db*) probes (*Center*, red). In the example shown, *Xist* RNA does not spread beyond the translocation breakpoint. (*B*) Representative examples of *Xist* RNA localization on 4^{X}i chromosomes in 3-day differentiating TMA-2/S8 ES cells. Cells are classified according to the same criteria as used in Fig. 2. Schematic on the left illustrates the extent of *Xist* RNA spread (green box), for each of the three categories. (*C*) Summary of *Xist* RNA analysis in 3-day differentiating TMA-2/S8 ES cells. Each category of cells is shown as a proportion of the total number of cells with a 4^{X}i chromosome. Data obtained for T37H fibroblasts published in ref. 19 are shown for comparison.

Xist RNA, the primary inactivating signal. TMA-2/S8 cells were differentiated for 3 days. This time point was the earliest from which we could obtain a reasonable number of metaphases from cells having initiated *Xist* RNA expression during the previous 24 h (Fig. 1*E*). In no case did we observe spreading over the entire 4^{X} chromosome (Fig. 3 *A*–*C*). The majority of examples showed either no spread or limited spread up to the *db*/*b* loci. A small proportion showed spread just beyond the *b* locus. Again, the results correlated almost exactly with our previous analysis of T37H fibroblasts (19), which is included in Fig. 3*C* for comparison. A small number of metaphases were obtained from 2-day differentiated cells, and, here also, there was very limited spread of *Xist* RNA into chromosome 4 material (data not shown). Collectively, these findings suggest that chromosome 4 sequences close to the breakpoint of the 4^{X} translocation product present a block to the initial spread of *Xist* RNA.

L1 Depletion on Chromosome 4 at the X;A Translocation Breakpoint. Based on recent studies suggesting L1 elements as candidates for the way stations that boost the inactivation signal (16–18), we wanted to determine L1 density in relation to the T37H translocation. We fine-mapped the translocation breakpoint on chromosome 4 to a region between Mb 142 and 143 by using DNA FISH analysis with bacterial artificial chromosome (BAC) clones (Fig. 4*A*). We then calculated the percentage of L1 content in 1-Mb segments along both the X chromosome and chromosome 4 in the mouse. The data are shown, together with gene density for the equivalent segments in Fig. 4*B*.

L1 content on the mouse X chromosome is high along most of the length of the chromosome, similar to the human X chromosome. On chromosome 4, L1 content is much more variable, with large domains, generally of 1–5 Mb, that have either a high or low density of L1 homologous sequence. Low-density L1 domains generally correspond to gene-rich regions, as has been noted in other studies (see, for example, refs. 31 and 32). Interestingly, the T37H breakpoint corresponds to the beginning of an exceptionally large gene-rich domain on chromosome 4, with low L1 density extending over ≈20 Mb (Fig. 4). This unusual feature, occurring precisely at the breakpoint site, could provide an explanation for attenuated spreading in T37H.

Discussion

In this study, we have assessed spread of *Xist* RNA and X inactivation in the T37H translocation at the onset of random X inactivation. Collectively, our data suggest that the initial spread of X inactivation is blocked close to the translocation breakpoint. An

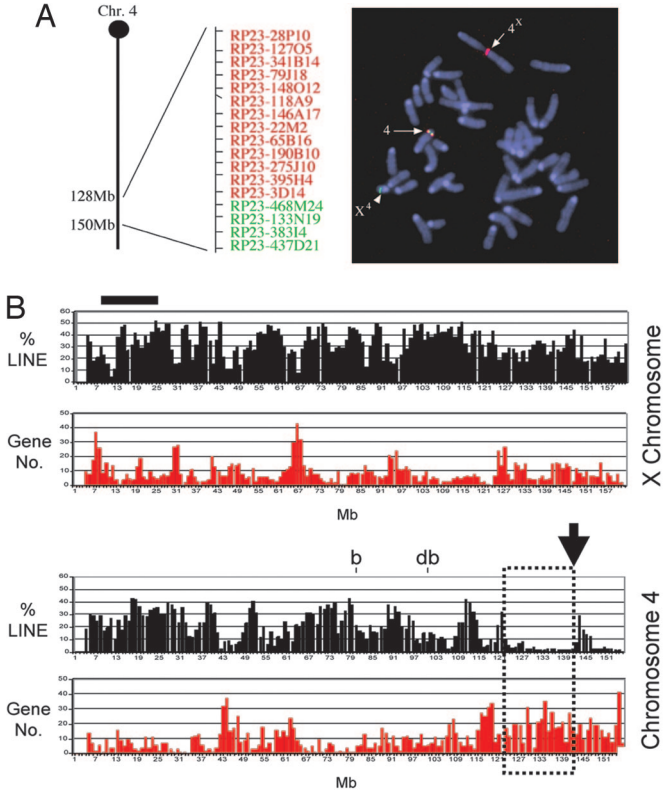

Fig. 4. A large gene-rich/LINE-1-poor domain at the translocation breakpoint correlates with restricted spreading of X inactivation. (*A*) Fine-mapping of the chromosome 4 breakpoint. Schematic shows an expanded view of the region on chromosome 4 between 128 and 150 Mb, with the location of BAC probes assigned to the 4^X (red) or X^4 (green) translocation product by using DNA FISH analysis. Example shows DNA FISH with BAC clones RP23–3D14 (red) and RP23–468M24 (green), spaced 1 Mb apart at 142 and 143 Mb on chromosome 4. (*B*) The figure illustrates LINE-1 (L1) homology as the percentage of total sequence (black bars) and the number of genes (red bars) in 1-Mb intervals along the entire length of chromosome X (*Upper*) and chromosome 4 (*Lower*). For the X chromosome, the location of the T37H breakpoint (cytogenetic band XA2, approximately Mb 15–32) is indicated with a thick black line. For chromosome 4, the precisely mapped position of the T37H breakpoint (142–143 Mb) is marked with the large arrow. The positions of the *b* and *db* loci are also shown. A 20-Mb L1-poor/gene-rich domain occurring at the breakpoint is highlighted with a dotted line. Data are extracted from Ensembl mouse genome sequence release m34.

exceptionally large 20-Mb low-density L1 domain, located at the breakpoint, provides a possible basis for attenuated spread.

In analyzing H3K27me3, we observed a small proportion of cases where spread appeared to have occurred over most of the 4^Xi product. Interestingly, this time point was at day 3 of differentiation, the earliest analyzed, raising the possibility that there is an initial chromosome-wide spread that retreats extremely rapidly. Although we cannot rule out this initial spread, we consider it unlikely for a number of reasons. First, the three examples of 4^X chromosomes showing near complete coverage with H3K27me3 had relatively condensed metaphase chromosomes, making it difficult to be certain at which point the spread terminated (see, for example, Fig. 2*B4*). Second, analysis of the kinetics of *Xist* induction demonstrated that a significant proportion of cells at the 3- and 5-day time points up-regulated *Xist* RNA within the preceding 24 h. We would, therefore, have expected to see a greater proportion of cells with complete spreading and, moreover, to see examples at the 5-day time point also. Finally, even if *Xist* RNA retreats relatively rapidly, for example, in just a few hours, we would expect the stable H3K27me3 chromatin modification to remain at least through a single cell-division cycle, marking the domains previously coated with *Xist* RNA. With these factors in mind, we think it more likely that the cases showing spread over most of the 4^X chromosome represent rare stochastic variations in which the factors that attenuate spreading have been less effective.

In this study, we used surrogate markers for *Xist*-induced silencing (i.e., spreading of *Xist* RNA and histone modifications), and the expression status of individual chromosome 4 loci on 4^Xi chromosomes remains an open question. Evidence from classical studies indicate that the *b* locus is silenced quite efficiently and, conversely, that misty (*m*), located between *b* and the translocation breakpoint, is not silenced. Models to explain discontinuous silencing were discussed in the context of our analysis of T37H adult fibroblasts (19).

The presence of a large domain with low L1 density at the T37H breakpoint provides a possible explanation for attenuated spreading. We observe both *Xist* RNA and silencing-associated chromatin modifications extending up to the *db*/*b* loci in a proportion of cells, suggesting that the L1-poor domain reduces the efficiency of spreading in a probabilistic fashion on a cell-to-cell basis. This hypothesis would be consistent with the observation that, on some metaphases, both X inactivation- and active transcription-associated chromatin modification marks (H3K27me3 and H4 acetylation, respectively) occur in the region between the breakpoint and the *db*/*b* loci (Fig. 2*D*).

How might L1 elements facilitate spread of *Xist* RNA? One possibility is that there is a direct interaction between *Xist* RNA and L1 elements, perhaps through proteins associated with the repeats. We consider this scenario unlikely because, in a previous study, we found that *Xist* RNA is concentrated over L1-poor G-light bands on the X chromosome (19). As an alternative, we propose a role for L1 elements in organizing the chromosome spatially, tethering gene-poor domains in large aggregates around the nuclear periphery. Where large L1-depleted domains occur, such as the 20-Mb region on chromosome 4, this organization could create a spatial separation of chromosome regions either side, which, in turn, could mediate against the efficient transit of *Xist* RNA.

In light of our findings, it is interesting to consider why spread of *Xist* RNA along autosomes is relatively efficient in *Xist* transgene experiments described to date (11, 12). A possible factor is that L1-poor/gene-rich domains as large as the 20-Mb domain we observe at the T37H breakpoint are relatively infrequent in the mouse genome (N.B., unpublished observation). Also of possible significance is that transgene *Xist* RNA often exceeds physiological levels, and this excess may aid spread over large L1-poor regions on the respective autosomes. These two possibilities are not mutually exclusive. It should be noted that evidence for an involvement of L1 elements in spread of X inactivation remains correlative, in both this study and elsewhere. Experiments that address this question directly are still required.

In summary, we provide direct evidence that *in cis* spread of *Xist* RNA at the onset of X inactivation can be attenuated by autosomal sequences. Clearly, this mechanism could account for other examples where *Xist*-mediated silencing of autosomal sequences is relatively inefficient. It should be borne in mind that failure to efficiently maintain silencing or spread and retreat must also contribute in at least some instances (10). Further investigation of the role of L1 elements will be interesting in terms of addressing the mechanisms operating in both cases.

Materials and Methods

Cell Culture. Establishment and characterization of TMA-2 ES cell line carrying the T(X;4)37H translocation has been described in ref. 24. The stable TMA-2/S8 subclone carrying a normal chromosome X and chromosome 4, 4^X, and X^4 translocation products was selected by subcloning and karyotype analysis. Undifferentiated TMA cells were grown on mitomycin-inactivated mouse embryonic fibroblasts in DMEM (GIBCO)

supplemented with 16% FCS (Autogen Bioclear, Calne, Wiltshire, U.K.), L-glutamine, nonessential amino acids, 50 IU/ml penicillin/streptomycin, 2-mercaptoethanol (GIBCO), and 1,000 units/ml LIF (Chemicon) at 37°C and 5% CO_2. ES cell differentiation was induced by withdrawal of LIF and feeder cells and low-density plating (1×10^4 cells per cm^2).

Immunofluorescence Analysis. Analysis of histone modifications was performed on TMA-2 cells cytospun onto Superfrost Plus glass slides (Cytospin centrifuge; Shandon, Pittsburgh). Because of fragility, TMA-2 cells had to be fixed before cytospinning. The procedure for cell preparation was as follows. Ethidium bromide (1 μg/ml final concentration; BDH) and colcemid (KaryoMax Colcemid solution, 0.1 μg/ml final concentration; GIBCO) were added to the cell culture 2 h before cell harvesting to increase the proportion of extended metaphases. Trypsinized cells were rinsed in PBS and swollen in hypotonic solution (75 mM KCl) for 10 min at room temperature (RT). Cells were fixed and permeabilized simultaneously by addition of equal volume of 2× GT buffer and incubation for 20 min at 37°C. GT buffer was essentially composed of stabilization buffer, pH 7.0 (33), with addition of glutaraldehyde (final concentration 0.02%; EMS) for fixation and Triton X-100 (final concentration 0.5%; Sigma) for permeabilization. Cells ($3–5 \times 10^4$) were cytospun at 2,000 rpm for 10 min in a cytofuge (Shandon, Pittsburgh), and slides were incubated in sodium borohydride (2 mg/ml in H_2O; Aldrich) for 15 min at RT to reduce the free aldehyde groups formed during glutaraldehyde fixation. After two washes in PBS and three washes in KCM buffer (10 mM Tris·HCl, pH 8/120 mM KCl/20 mM NaCl/0.5 mM EDTA/0.1% Tween 20), 10 min each, slides were blocked for 30 min at RT in normal goat serum (NGS, 10% vol/vol; Sigma) and BSA (2.5% wt/vol; NEB) diluted in KCM buffer. Monoclonal antibody specific for di/tri-methylated H3K27 (gift from D. Reinberg, University of Medicine and Dentistry of New Jersey, Piscataway, NJ) or polyclonal H4 acetylated (Penta) antibody (Upstate Biotechnology, Lake Placid, NY) was then applied for 1–2 h at RT, and the slides were washed again in KCM buffer three times for 5 min and then incubated with secondary antibody (Alexa Fluor 488 goat anti-mouse or Alexa Fluor 568 goat anti-rabbit; Molecular Probes) for 1 h at RT. For double staining of H3K27me3 and H4Ac, the slides were incubated simultaneously in both primary antibodies, followed by detection with secondary antibodies. After three 5-min washes in KCM buffer and a brief rinse in PBS, slides were mounted in Vectashield mounting medium (Vector Laboratories) containing DAPI counterstain. Images were captured on a Leica DMRB fluorescence microscope by using a Photometrics charge-coupled device camera and QUIPS software (Applied Imaging, San Jose, CA).

RNA FISH. RNA FISH was performed essentially as described in refs. 34 and 35, with some modifications. Briefly, trypsinized cells were fixed and permeabilized simultaneously (4% formaldehyde/5% glacial acetic acid/0.9% NaCl/0.5% Triton X-100) for 10 min at 4°C. Cells ($3–5 \times 10^4$) were cytospun at 2,000 rpm for 10 min in a Shandon cytofuge, and the slides were rinsed twice in PBS for 5 min each time. Ready-to-use slides were either used for RNA FISH immediately (34, 35) or stored in 70% ethanol at 4°C until use. Digoxygenin-11-dUTP- (Roche) labeled *Xist* plasmid covering the whole *Xist* cDNA region was used as a probe. The probe was detected with antidigoxygenin fluorescein isothiocyanate (AD-FITC) antibody raised in sheep (Roche), followed by anti-sheep FITC antibody (Vector Laboratories). Combined RNA/DNA FISH was performed as described in ref. 19.

The translocation breakpoint on mouse chromosome 4 was mapped by DNA FISH hybridization of 17 BAC clones (BACPAC Resources, Children's Hospital Oakland Research Institute, Oakland, CA) spanning the region between 128 and 150 Mb to TMA-2 metaphase spreads. BAC clones were labeled with digoxygenin-11-dUTP or biotin-16-dUTP (Roche) and hybridized in pairs. DNA FISH and probe detection was performed essentially as described in ref. 36. Positions of BAC clones mapped to the 4^X translocation product are shown in Fig. 4.

Estimation of Distance of Spread on 4^Xi Chromosomes. DNA FISH markers on the X chromosome and chromosome 4 were used to assess the spread of H3K27me3, H4 acetylation, and *Xist* RNA. These markers were the DXCrc141 repeat sequence island located on the X chromosome close to the X translocation breakpoint, BAC clones mapping to the diabetes (*db*) locus, ≈20 Mb proximal of the X;A breakpoint on chromosome 4, and BAC clones mapping to the brown (*b*) locus, ≈30 Mb proximal of the X;A breakpoint. Mapping was further facilitated by the occurrence of a primary constriction localizing to the region of the translocation breakpoint. Metaphase chromosomes were analyzed only where we could clearly discern the different markers that were required for scoring.

We thank members of the Developmental Epigenetics group, K. E. Brown and A. Saveliev for helpful discussion and input, and Danny Reinberg for the gift of 2/3meH3K27 antibody. This work was funded by the Medical Research Council, United Kingdom.

1. Heard, E., Clerc, P. & Avner, P. (1997) *Annu. Rev. Genet.* **31,** 571–610.
2. Brown, C. J., Ballabio, A., Rupert, J. L., Lafreniere, R. G., Grompe, M., Tonlorenzi, R. & Willard, H. F. (1991) *Nature* **349,** 38–44.
3. Brockdorff, N., Ashworth, A., Kay, G. F., McCabe, V. M., Norris, D. P., Cooper, P. J., Swift, S. & Rastan, S. (1992) *Cell* **71,** 515–526.
4. Brown, C. J., Hendrich, B. D., Rupert, J. L., Lafreniere, R. G., Xing, Y., Lawrence, J. & Willard, H. F. (1992) *Cell* **71,** 527–542.
5. Penny, G. D., Kay, G. F., Sheardown, S. A., Rastan, S. & Brockdorff, N. (1996) *Nature* **379,** 131–137.
6. Lee, J. T., Strauss, W. M., Dausman, J. A. & Jaenisch, R. (1996) *Cell* **86,** 83–94.
7. Herzing, L. B., Romer, J. T., Horn, J. M. & Ashworth, A. (1997) *Nature* **386,** 272–275.
8. Heard, E. (2004) *Curr. Opin. Cell Biol.* **16,** 247–255.
9. Russell, L. B. (1963) *Science* **140,** 976–978.
10. Cattanach, B. M. (1974) *Genet. Res.* **23,** 291–306.
11. Lee, J. T. & Jaenisch, R. (1997) *Nature* **386,** 275–279.
12. Wutz, A. & Jaenisch, R. (2000) *Mol. Cell* **5,** 695–705.
13. Rastan, S. (1983) *J. Embryol. Exp. Morphol.* **78,** 1–22.
14. Shao, C. S. & Takagi, N. (1991) *Jpn. J. Genet.* **66,** 433–447.
15. Gartler, S. M. and Riggs, A. D. (1983) *Annu. Rev. Genet.* **17,** 155–190.
16. Lyon, M. F. (1998) *Cytogenet. Cell Genet.* **80,** 133–137.
17. Bailey, J. A., Carrel, L., Chakravarti, A. & Eichler, E. E. (2000) *Proc. Natl. Acad. Sci. USA* **97,** 6634–6639.
18. Ross, M. T., Grafham, D. V., Coffey, A. J., Scherer, S., McLay, K., Muzny, D., Platzer, M., Howell, G. R., Burrows, C., Bird, C. P., *et al.* (2005) *Nature* **434,** 325–337.
19. Duthie, S. M., Nesterova, T. B., Formstone, E. J., Keohane, A. M., Turner, B. M., Zakian, S. M. & Brockdorff, N. (1999) *Hum. Mol. Genet.* **8,** 195–204.
20. White, W. M., Willard, H. F., Van Dyke, D. L. & Wolff, D. J. (1998) *Am. J. Hum. Genet.* **63,** 20–28.
21. Keohane, A. M., Barlow, A. L., Waters, J., Bourn, D. & Turner, B. M. (1999) *Hum. Mol. Genet.* **8,** 377–383.
22. Sharp, A. J., Spotswood, H. T., Robinson, D. O., Turner, B. M. & Jacobs, P. A. (2002) *Hum. Mol. Genet.* **11,** 3145–3156.
23. Hall, L. L., Clemson, C. M., Byron, M., Wydner, K. & Lawrence, J. B. (2002) *Hum. Mol. Genet.* **11,** 3157–3165.
24. Tada, T., Tada, M. & Takagi, T. (1993) *Development (Cambridge, U.K.)* **119,** 813–816.
25. Searle, A. G., Beechey, C. V., Evans, E. P. & Kirk, M. (1983) *Cytogenet. Cell Genet.* **35,** 279–292.
26. Zvetkova, I., Apedaile, A., Ramsahoye, B., Mermoud, J. E., Crompton, L. A., John, R., Feil, R. & Brockdorff, N. (2005) *Nat. Genet.* **37,** 1274–1279.
27. Sheardown, S. A., Duthie, S. M., Johnston, C. M., Newall, A. E., Formstone, E. J., Arkell, R. M., Nesterova, T. B., Alghisi, G. C., Rastan, S. & Brockdorff, N. (1997) *Cell* **91,** 99–107.
28. Silva, J., Mak, W., Zvetkova, I., Appanah, R., Nesterova, T. B., Webster, Z., Peters, A. H., Jenuwein, T., Otte, A. P. & Brockdorff, N. (2003) *Dev. Cell* **4,** 481–495.
29. Kohlmaier, A., Savarese, F., Lachner, M., Martens, J., Jenuwein, T. & Wutz, A. (2004) *PLoS Biol.* **2,** e171.
30. Mak, W., Baxter, J., Silva, J., Newall, A. E., Otte, A. P. & Brockdorff, N. (2002) *Curr. Biol.* **12,** 1016–1020.
31. Boyle, A. L., Ballard, S. G. & Ward, D. C. (1990) *Proc. Natl. Acad. Sci. USA* **87,** 7757–7761.
32. Cross, S. H., Lee, M., Clark, V. H., Craig, J. M., Bird, A. P. & Bickmore, W. A. (1997) *Genomics* **40,** 454–461.
33. Rudnicki, M. A. & McBurney, M. W. (1987) in *Teratocarcinomas and Embryonic Stem Cells: A Practical Approach*, ed., Robertson, E. J. (IRL, Oxford), pp. 19–49.
34. Lawrence, J. B., Singer, R. H. & Marselle, L. M. (1989) *Cell* **57,** 493–502.
35. Clerc, P. & Avner, P. (1998) *Nat. Genet.* **19,** 249–253.
36. Nesterova, T. B., Duthie, S. M., Mazurok, N. A., Isaenko, A. A., Rubtsova, N. V., Zakian, S. M. & Brockdorff, N. (1998) *Chromosome Res.* **6,** 41–48.